Preparation and Characterization of Poly(acrylamide/maleic acid)-based hydrogels Composites

Poli(akrilamid-maleik asit) temelli hidrojel kompozitlerin Hazırlanması ve Karakterizasyonu

Research Article

Recep Akkaya* and Ulvi Ulusoy
Cumhuriyet University, Department of Chemistry, Sivas, Turkey

ABSTRACT

The principle aim of this investigation was the preparation and characterization of the composites formed from Bentonite (B) and Zeolite (Z) minerals, and polyacrylamide-co-maleic acid (PAA-MA) hydrogel polymers. The procedures used in obtaining the polymers were also applied in preparation of the composites by direct polymerization of the monomers of interests dissolved in the suspension of B or Z. The prepared PAA-MA and the composites were characterized with the data and analysis results obtained from FT-IR, TGA, SEM, BET-porosity and Zero Point of Surface Charge (PZC). The results of FT-IR, TGA, SEM, BET-porosity and PZC analysis presented certain evidences for the formation of composites, it was impressed that the composites were the mixtures composed of two phases composing of organic (PAA-MA) and inorganic (B or Z) phases rather than the formation of polymer/mineral hybrid.

Key Words
Composite, Polyacrylamide-co-Maleic Acid, Bentonite, Zeolite

ÖZET

Bu araştırmanın temel amacı Bentonit (B) ve Zeolit (Z) minerallerinin hidrojel polimer olan Poliakrilamid-ko-maleik asit (PAA-MA) ile oluşturduğu kompozitini hazırlamak ve karakterize etmektir. Polimerlerin elde edilmesinde kullanılan yöntem, kompozitlerin hazırlanmasında da kullanılmış ve B veya Z içeren süspansiyon ortamında bulunan ilgili monomerlere doğrudan polimerleştirme işlemi uygulanmıştır. Hazırlanan PAA-MA ve kompozitlerin yapısal karakterizasyonunda FT-IR, TGA, SEM, BET-Gözeneklilik ve sıfır yüzey yük noktası (PZC) ile ilgili veri ve analiz sonuçları kullanılmıştır. FT-IR, XRD, TGA, SEM, BET-gözeneklilik ve PZC analiz sonuçları kompozit oluşumu ile ilgili kesin kanıtlar sunmuş, yapıların polimer/mineral hibrit oluşumundan çok biri organik (PAA-MA) ve diğeri inorganik özellikteki (B veya Z) iki faz içeren bir karışım olduğu kanısına varılmıştır.

Anahtar Kelimeler
Kompozit , Poliakrilamid-ko-Maleik asit, Bentonit, Zeolit

Article History: Received March 3, 2011; Revised October 25, 2011; Accepted November 18, 2011; Avaliable Online: December 02, 2011.

Correspondence to: Recep AKKAYA, Cumhuriyet University, Department of Chemistry, Sivas, Turkey
Tel: +90 346 2191010 Ext: 1568 Fax: +90 346 2191186 E-Mail: recepakkaya5835@gmail.com
rakkaya@cumhuriyet.edu.tr

INTRODUCTION

Hydrogels are three-dimensional networks of hydrophilic polymers capable of retaining large amounts of water or biological fluids within their structure. The networks are composed of homopolymers or copolymers, and are insoluble due to physical or chemical crosslinks. Their strong water absorbance and rubbery nature resemble natural tissues, and they have good biocompatibility and biological inertness. Hydrogels can be non-toxic, chemically stable and can be exhibit a low interfacial tension with aqueous environments. Hydrogels are good candidates for preparing biomedical materials such as: contact lenses, wound dressing, membranes for biosensors, and linings for artificial heart [1,2]. The hydrogels based polyelectrolyte structures are crosslinked hydrophilic polymers capable of swelling retain water without dissolving. PAA-MA hydrogels copolymers are highly hydrophilic, neutral but are not reusable [3]. The swelling of PAA-MA is important problem about the studying of column techniques and metal adsorption.

In recent years, considerable researches have been done on the characterization and swelling behaviour of hydrogels prepared by simultaneous free radical copolymerization and crosslinking in the presence of an initiator and a crosslinking agent [4]. Superswelling hydrogels exhibit a combination of unique physicochemical properties, thus permitting their wide-ranging, and often exceptional, possibilities in practical applications [4]. In recent studies, hydrogels–clay and zeolite nanocomposites have attracted much attention in many fields of polymer industry due to improved mechanical, thermal, barrier and fire retardant properties, dimensional stability compared with the pure polymer or conventional composites [5]. Recently, polymer/clay composite hydrogels have been studied to improve the properties of hydrogel, such as mechanical strength, swelling and deswelling properties. For example, Messersmith and Znidarsich [6] prepared stimuli-responsive hydrogel/clay composites by polymerization of aqueous suspension composed of N-isopropylacrylamide, N,NO-methylene bisacrylamide and Na-montmorillonite. Wu et al. [7,8] reported the preparation of starch-g-polyacrylamide/clay and poly(acrylic acid)/mica composites with striking capability of water absorption by grafting the monomers on the inorganic clay/mica. Zhang et al. [9] synthesized nano-composite hydrogel (abbreviated as NC hydrogels) with high thermal stability and swelling ratio by grafting acrylic acid on the organophilic montmorillonite. Haraguchi's group obtained poly (N-isopropylacrylamide)/clay [10,11] and poly(N, N-dimethylacrylamide)/clay NC hydrogels [12] with much improved mechanical properties using modified clay as the cross-linker [13].

In previous articles, the composites of natural bentonite and zeolite) with polyacrylamide-maleic acid (PAA-MA) were synthesized and characterized by FT-IR, TGA, XRD and SEM analysis.

The purpose of this study was to prepare and characterize polyacrylamide-maleic acid P(AA-MA) hydrogel and composite modified with bentonite and zeolite. Dynamic swelling studies are important for swelling characterization of composites systems. These swelling properties will be effected that usable of its as biomaterial in medicine, pharmacy and veterinary. Also, the long-term stability, physical and swelling properties, and sterilization were investigated. In this work, it has been aimed to study a convenient method for removing the water-soluble monovalent metal ions from aqueous solutions by adsorption on novel composite adsorbent such as P(AAm-MA-B) and P(AA-MA-Z) composites.

EXPERIMENTAL

Reagents

Na-montmorillonite (bentonite) in 98% purity (with a cation exchange capacity, CEC of 0.8 mol/kg) was purchased from SigmaAldrich. The Zeolite mineral is composed of ~90% zeolite, as clinoptilolite $\{(Na,K)_6.[Al_6Si_{30}O_{72}].24H_2O\}$ and mordenite $\{Na_3KCa_2.[Al_8Si_{40}O_{96}].28H_2O\}$, 5% quartz, 5% feldspar and smectite in trace level. The ratio of SiO_2/Al_2O_3 is 4.7, which suggests that the zeolite is clinoptilolite with reference to the classification of International Mineralogical Association. The univalent cation exchange capacity (CEC) zeolite was 1.64 meq/g [14]. The zeolite rocks were crashed, ground and sieved to 100 mesh size. No pre-treatment was applied to the chemicals, clay and zeolite.

Acrylamide (AA) and maleic acid (MA), monomers, the activator N,N'-methylene-bisacrylamide, N,N,N',N'-tetramethylethylene-diamine (TEMED), the initiator, ammonium peroxodisulfate APS ($H_8N_2O_8S_2$), 4-(2-pyridylazo) resorcinol (PAR), Arsenazo III (disodium salt) were purchased from Sigma. All chemicals used were of analytical reagent grade.

All experiments were always performed in duplicates. ±5% was the limit of experimental error of each duplicates, any experiment resulted in higher than this limit was repeated.

Preparation of PAA-MA, PAA-mA/B and PAA-MA/Z

Preparation of hydrogels (PAA-MA)

In the first part of this study, PAA-MA hydrog els were synthesized by bulk copolymerization of AA and MA using N,N,N',N'-tetramethyl-ethylenediamine as the crosslinker. APS and TEMED were used as an initator and an activator, respectively. The solution containing AA (4 g), MA (0.36 g), N,N,N',N'-tetramethylethylenediamine (1.2 g), APS (4 mL) and TEMED (800 μL) were prepared in 40 mL water mixture [15].

PAA-MA hydrogels were synthesized with different AA-MA ratios by using water as cross-linking agent by bulk polymerization. Maleic acid amount 20, 30, 40, 50, 60, 70, 80, 90 and 100 mg were each added to the solutions of monomers of 1 g AA. Hydrogels obtanied from these systems are denoted as PAA-MA 1, 2, 3, 4, 5, 6, 7, 8 and 9 respectively. PAA-MA-8 was adsorbed as the optimum. PAA-MA hydrogels was washed after completion of the polymerization with distilled water until the effluent attained neutral pH. The gel was dried at ambient temperature, ground and sieved to a particle size smaller than 25 mesh, and stored in polypropylene container.

Polymer and/or residual monomers were removed from the gel structure by this extraction. The amount of MA in the monomer, polymer and/or copolymer form was determined by titration of extract against NaOH (0.1 M) to a phenolphthalein end point, but no titrate was consumed for all PAA-MA hydrogels reaching 100% conversion [15-17].

Preparation of modified PAA-MA hydrogels (PAA-MA/B and PAA-MA/Z)

For preparation of 6 g of PAA-MA/B; 4 g of B or Z in 20 mL of water was stirred for 15 min to obtain a homogeneous suspension. 10 mL of solution containing 0.135 g maleic acid, 20 mL of solution containing 1.5 g of acrylamide monomer to provide a mass ratio 2:1 was added to the suspension and stirred additional 4 hours. 2 mL of N,N'-methylenebisacrylamide as cross linking agent and 50 mg ammoniumpersulphate dissolved in 10 mL distilled water was contained on to the suspension. Finally, 200 μL of N,N,N',N'-tetramethylethylenediamine was added to propagate the polymerization at 25°C. PAA-MA/B or PAA-MA/Z composites were washed after completion of the polymerization with distilled water until the effluent attained neutral pH. The composites were dried at ambient temperature, ground and sieved to a particle -25 mesh size, and stored in polypropylene container [18].

Characterisation of hydrogel and composites

The procedures used in obtaining the polymers were also applied in preparation of the composites by direct polymerization of the monomers of interests dissolved in the suspension of B and Z. The prepared B, Z and PAA-MA and the composites (PAA-MA/B and PAA-MA/Z) were characterized with the data and analysis results obtained from FT-IR, XRD, TGA, SEM, BET-porosity, Swelling studies and Zero Point of Surface Charge (PZC).

Fourier transform infrared spectroscopy (FT-IR)

FT-IR spectrometric (Mattson 1000, UK) analysis was used to characterize the chemical structure of B, PAA-MA, PAA-MA/B, Z and PAA-MA/Z. All samples were prepared as KBr Pellets and spectra were taken at a resolution of 4 cm^{-1} and 5 times scanning in the frequency range 4000-400 cm^{-1}.

X-ray diffraction (XRD)

The X-ray diffraction patterns of composites and components were recorded using a Rigaku Dmax 2200 diffractometer equipped with Ni-filtered, a proportional counter, 2θ/min scan rate, using Cu K_α radiation (λ = 1.5418 Å). Dried particles were mounted on a sample holder and the patterns were recorded in the range of 10–50. at the speed of 5 m/min to know the crystallinity.

Thermal properties (TGA-DSC)

Thermal properties of the B, Z, PAA-MA, PAA-MA/B and PAA-MA/Z were investigated by using TGA (Shimadzu TA-50 thermogravimetric analyzer) and DSC techniques. The decomposition temperature measurements by TGA were carried out on 10±1 mg samples under a static air atmosphere at a heating rate of 100 °C/min from 25 °C to 600 °C.

Scanning electron microscopy (SEM)

The surface morphology of the composites and components were examined using scanning electron microscopy (SEM). Analysis of the composites (PAA-MA/B and PAA-MA/Z) and their components (B, Z, PAA-MA) SEM was obtained by means of SEM JEOL/JSM-6335F in Tubitak/Gebze Laboratories. The composites and components were coated with a thin layer of gold under reduced pressure and their SEM images were taken.

Surface area measurements (BET)

The specific surface area and micropore volume of the composites and components were determined by physical adsorption of nitrogen with the BET method at 77 K temperature using a Micromeritics ASAP 2400 automatic analyzer. The average size and size distribution of the composites and components were determined by screen analysis performed by using Tyler Standart sieves (Quantachrome Instruments).

Swelling studies

In order to determine the swelling behavior, 1 g of dry composites and components were placed into distilled water and kept at a constant temperature of 25 ± 0.5°C. Swollen composites and components were periodically removed and weight by an electronic balance. The weight ratio of dry and swollen samples were recorded. The water content of the swollen composites and components were calculated using the following expression:

$$\text{Swelling ratio (\%)} = [(w_f - w_o) / w_o] \times 100 \quad (1)$$

Where w_o and w_f are the weight of composites and components before and after swelling, respectively [12].

pH at the point of zero charge (PZC)

The pH at the point of zero charge (pHPZC) of the composites, namely the pH value required to give zero net surface charge, was measured using mass titration method [19-21]. For the measurement of the pHPZC, eleven solutions with different initial pH values, range of pH=1-11, were prepared with addition of 0.1 M aqueous solution of HNO_3 or KOH. KNO_3 was used as the background electrolyte. 0.1 g adsorbents of 10 mL of (initial pH 1-11) solution is added and mixed at room temperature. Finally, after 24 h, the pH of each solutions were measured with a pH meter CG 840B Schott. A plot of the equilibrium pH versus composites yields a curve showing a plateau and the pHPZC is identified as the point at which the change of pH is zero. The pHPZC is then taken as the average of the pH values.

RESULTS AND DISCUSSION

Structural evaluation

Fourier transform infrared spectroscopy (FT-IR)

The FT-IR spectra of the hydrogel and composites (PAA-MA, PAA-MA/B and PAA-MA/Z) and their components (B, Z) were compared in Figure 1 (a-b-c).

The spectra of PAA (Figure 1a) had clear counters around 3200 and 1560 cm^{-1} of NH_2, 1680 cm^{-1} of C=O of amide and 2900 cm^{-1} of C-H [22].

FT-IR spectra of MA, PAA and PAA-MA were evaluated, as presented in Figure 1. In these spectra, the stretching vibration bands appearing in the wave-number range 2400-3500 cm^{-1} were due to NH_2 and COOH groups in PAA-MA hydrogel.

This wide wave-number ranges made it a broad band due to some intramolecular hydrogen bonding in the copolymer. When MA is introduced into this copolymer, these peaks have increased in its intensity gradually with the increasing of COOH groups of maleic acid. The peak at 1750 cm^{-1} appears and characteristic for carbonyl group (C=O) stretch for both amide ($CO-NH_2$) and carboxylic (COOH) groups absorption and its intensity increased with incorporation of maleic acid to both hydrogels.

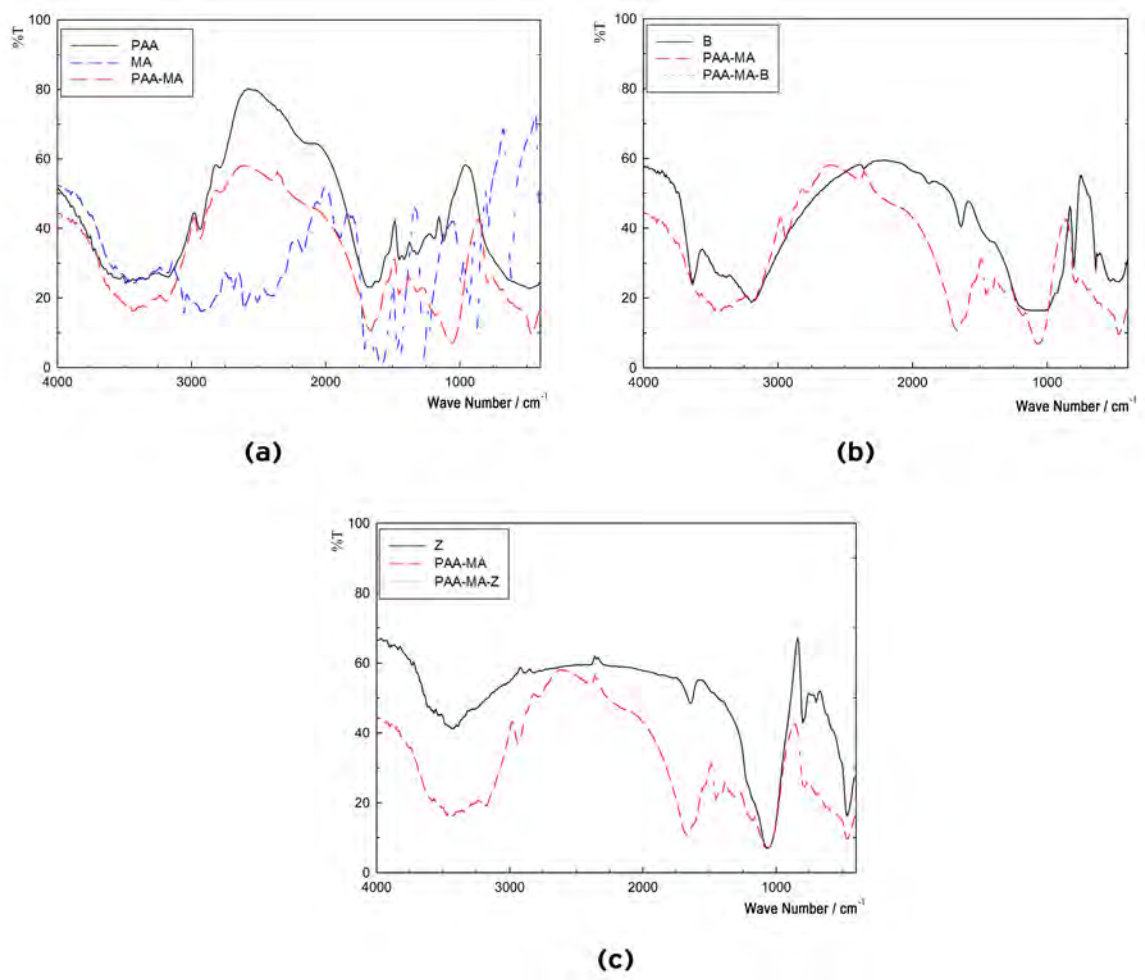

Figure 1. The comparasion of FT-IR spectra of PAA, MA and PAA-MA (a); B, PAA-MA ve PAA-MA-B (b) and Z, PAA-MA and PAA-MA-Z (c)

Table 1. B and PAA-MA/B is the characteristic reflections observed.

B			PAA-MA/B		
2θ/°	relative intensity %	FWHM/°	2θ/0	relative intensity %	FWHM/°
7.13_{001}	100	0.837	6.15_{001}	100	0.716
19.94_{002}	68	0.711	19.82_{002}	52	0.607

Table 2. Calculated with Bragg and Debye-Scherer distance between the layers and crystal size.

Bragg; d_{hkl} /nm			Debye-Scherer; d_{hkl} /nm		
B	PAA-MA-B	Δ*	B	PAA-MA-B	Δ*
124_{001}	144_{001}	20	95_{001}	111_{001}	16
			114_{002}	133_{002}	19
*Av.±SH			*105±9.5	122±11	18±1.5

Δ* = Δ[(PAA-MA-B)-B]

This band shifted to left frequencies as appeared at 1750 to 2200 due to the steric strain effect on anhydride structure which may be formed by water dehydration. Cyano group (C-N) on the chains of PAA-MA give absorption band at 1450 cm^{-1} while the peak at 1200 cm^{-1} can be attributed to (C-C) stretching vibration along the copolymeric chain structure [23]. The very important difference, in the result of FT-IR for the prepared hydrogel was seen the vinyl (C=C) which appeared at 1640 cm^{-1} streatching vibration for PAA-MA spectrum [23].

FT-IR spectra of PAA-MA, B and PAA-MA/B were evaluated, as presented in Figure 1b. The bands characterizing 'B' were the bending of Si-O-Si and Si-O-Al plane at 470 and 530 cm^{-1}, and the vibrations associated with R-O-Si (R=Al, Mg or Li) at 620 cm^{-1} and Si-O at 160-1120 cm^{-1} (broad band).

Bentonite, characteristic absorption peaks which indicate OH stretching of water molecules in the bentonite structure, OH groups between octahedral and tetrahedral sheets, and OH groups on the octahedral sheet were observed at 3425 cm^{-1} and 3680 cm^{-1}, respectively. Other characteristic peaks originating from the Si-O stretching at 1034 cm^{-1}, Al_2OH bending at 468 cm^{-1} were also observed [24].

In the spectrum of the composite, all the characteristic peaks of bentonite and PAA-MA/B composite were observed. PAA-MA/B composite structure, absorption peaks which indicate OH groups at 3600 cm^{-1} (in bentonite) disappeared. This result shows, it is supposed that the polymerization was occured on the bentonite layers. This research was explained by several researchers [5-25].

FT-IR spectra of PAA-MA, Z and PAA-MA/Z were evaluated, as presented in Figure 1c. The appearances of these counters together with the typical vibrations related to C=O , N-H, C-H terminals of PAA were of evidences for the hybrid formation of PAA-MA/Z. Beside the defined peaks of PAA-MA/Z, the appearances of the stretches belonging to Z [1215 and 1060 cm^{-1} of the $TO \rightarrow O$ and 800 cm^{-1} of Si-O-Si bridge] and the overall profiles of Z in PAA-MA/Z confirmed the hybrid formation of the composites. This might signify that there is interfacial interactions between the siloxane oxygen atoms or hydroxylated edges on the basal surface of the Z with PAA-MA.

X-ray diffraction (XRD)

In Figures 2-3, X-ray diffraction (XRD) patterns of the PAA-MA/B composites was compared with that of the bentonite.

The peak at 2θ=12.4 could be attributed to specific d_{001} basal spacing of montmorillonite phases of the bentonite (Table 1). Using XRD spectrum of B and PAA-MA/B with the openings between the layers were calculated by the Bragg equation; to explain; dhkl 'nm' as defined by Miller is the opening between bentonite layers; λ is the wavelength (0.154 nm); θ is the diffraction angle (^{0}); and n is an integer that denotes the order of the diffraction band. Only first order (n=1) diffraction bands are considered here.

Table 3. Z and PAA-MA/Z is the characteristic reflections observed in (Z for %10 relative intensity the of peaks that have not been evaluated under).

	Z			PAA-MA-Z		
Peak Number	2θhkl/^{0}	Relative Int./%	FWHM/^{0}	2θhkl/^{0}	Relative Int./%	FWHM/^{0}
1	6.50	10	0.332	6.58	46	1.880
2	9.78_{020}	14	0.239	8.88	-	-
3	13.46	13	0.277	13.34	-	-
4	19.65	11	0.213	19.85	34-	0.440
5	20.88	18	0.194	20.89	51	0.167
6	22.31_{004}	24	0.274	22.52	-	-
7	25.65	34	0.226	25.62	7	0.120
8	26.36	19	0.338	26.36	7	0.080
9	26.66	100	0.173	26.65	100	0.182
10	27.74	17	0.487	27.89	8	0.107

d_{001} openings of bentonite and PAA-MA/B are calculated as 12.4 Å (124 nm) and 14.4 Å (144 nm), respectively. On the other hand, peaks observed, at around 2θ = 6.15°, 7.13° in both bentonite and composites (B and PAA-MA/B), could be assigned to d_{001} spaces of expanded bentonite layers (Table 2). This indicates intercalation of polymer chains into bentonite layers and resulting in expanded interlayers spacing of 2 Å (20 nm). The expansion mechanism probably originates from the growing polymer chains by adsorbed monomers on the bentonite layers pushing apart the layers even in high bentonite loadings [5].

The crystallite size of B and Z was derived from Scherer's formula;

$$d_{hkl} = 0.9\ K_{\alpha} / (FWHM \cos \theta) \qquad (2)$$

where d_{hkl} is the crystallite size (nm), K is the wavelength of X-ray beam (0.15406 nm), FWHM is the full with at half maximum (rad) of the considered typcial reflection angle (0) with refference to the Miller indices at [L_{001}] and [L_{002}]. Debye Scherer should indicate the presence of between zeolite and PAA-MA.

The amorphous structure of PAA-MA/Z caused intense increase in the background. Indeed, growth, between layers of open platforms for evaluating d_{001} dramatically as 16 nm was observed. A revealing feature in the synthesis of the PAA-MA/Z was strong correlation between the Z and PAA-MA of the Bragg and Scherer equation of resulting (Tables 3-4). Z crystal size because of the large 100 nm in the PAA-MA/Z, composite obtained by Alexandre and Dubois (2000) classification according to the different micro-phase composite was considered.

Thermal properties (TGA-DSC)

Thermal stability of the materials have been determined by thermogravimetric studies. This technique reveals the loss of mass of a given substance during the heating process, and in this way information on the type of interactions between the hydrogel and B, Z can be obtained. Furthermore the DTG curves of each heating process were evaluated. An example is shown in Figures 4-5. The thermogravimetric parameters for all the samples are summarized in Tables 5-8.

The thermogravimetric curves of different PAA-MA reveal that there are there distinct steps of weight loss. It was suggested that the initial stage of thermal

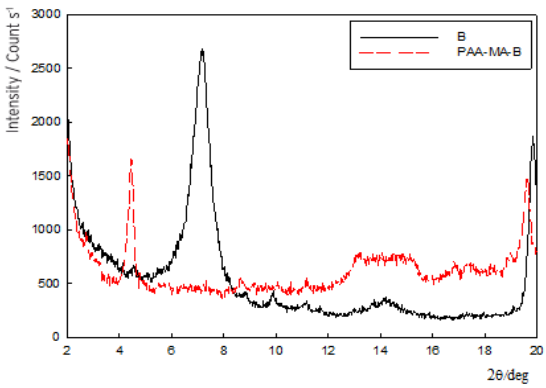

Figure 2. XRD spectra of B (lower spectrum) and PAA-MA/B.

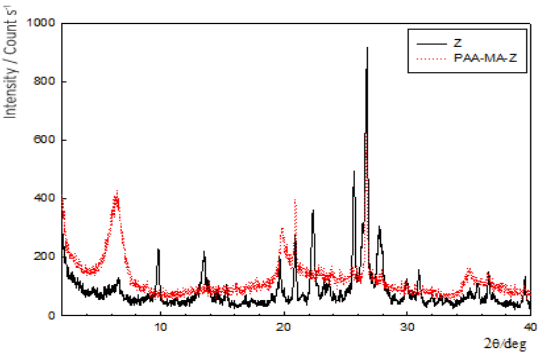

Figure 3. XRD spectra of Z (lower spectrum) and PAA-MA/Z.

Table 4. Calculated using the Debye-Scherer equation of Z and PAA-MA/Z crystal size (d_{hkl}/nm) and differences.

Peak Number	Z	PAA-MA-Z	Δ[(PAA-MA-Z)-Z]
1	240	42	-198
2	334_{020}	-	-
3	288	-	-
4	379	183	-196
5	417	484	67
6	295_{004}	-	-
7	360	679	319
8	242	1020	778
9	472	448	-24
10	168	765	597

Table 5. Derivative TGA analysis of B, PAA-MA and PAA-MA/B of temperature range.

Materials	Loss of Mass (% (W/V)				
	25-100°C	100-200°C	200-400°C	400-600°C	25-600°C
B	4,6	0,2	0,3	2,7	7,8
PAA-MA	9,2	3,3	41,5	29,2	83,3
PAA-MA/ B	7,1	2,5	23,5	21,6	54,6

Table 6. Mass loss and DTG result of B, PAA-MA ve PAA-MA-B.

Materials	DTG /°C
B	54
PAA-MA	326
PAA-MA/B	312

Table 7. Derivative TGA analysis of Z, PAA-MA ve PAA-MA-Z of temperature range.

Materials	25-100°C	100-200°C	200-400°C	400-600°C	25-600°C
Z	3,3	3,3	2,3	0,8	9,7
PAA-MA	9,2	3,3	41,5	29,2	83,3
PAA-MA/Z	6,3	1,0	27,3	9,7	44,3

Table 8. Mass loss and DTG result of Z, PAA-MA and PAA-MA/Z.

Materials	DTG /°C
Z	94
PAA-MA	326
PAA-MA/Z	334

Table 9. Physical characteristics of PAA-MA, B, PAA-MA/B, Z and PAA-MA/Z.

	BET surface area /m^2g^{-1}	Pore volume /cm^3g^{-1}	Pore diameter /nm
PAA-MA	1,8	0,015	1,44
B	33,4	0,178	0,44
PAA-MA-B	5,9	0,078	0,48
Z	10,4	0,071	0,44
PAA-MA-Z	4,6	0,038	0,53

Table 10. B, Z, PAA-MA, PAA-MA-B ve PAA-MA-MA-Z composites and swelling capacities of components

Materials	Swelling capacity, %
B	1150
Z	15
PAA-MA	1035
PAA-MA-B	3340
PAA-MA-Z	1340

Table 11. Acid/Base titration and pH_{pzc} of the PAA-MA, PAA-MA/B ve PAA-MA/Z used in study.

	PZC	R^2
PAA-MA	6,2	0,997
PAA-MA-B	6,5	0,982
PAA-MA-Z	6,0	0,983

* Linearity consistency coefficient; statistically significant, $p < 0.05$

diagram in the range from ambient temperature to 220°C the weight loss is due to dehydrationprocess of the water contained in such hydrophilic PAA-MA. At the second stage from 220°C to 340°C, to loss of the NH_3 by imidization. However, at the third stage above 340°C, the weight loss is due to the the main chain scission in the PAA-MA. This degradation was explained by several researchers before [23-28]. It was observed that Tmax of PAA-MA hydrogel is lower than that of PAA-MA/B and PAA-MA/Z composites. So it is said that, PAA-MA hydrogel in the case of adding B rapidly increased with the heat resistance. PAA-MA/B and PAA-MA/Z have been a higher thermal stability than PAA-MA.

Scanning electron microscopy (SEM)

The SEM photographs of the composite and its components were compared in Figures 6-7. Obvious change in PAA-MA morphology by introduction of B and Z should also be evidence for the composition of PAA-MA/B and PAA-MA/Z were the hybrids of PAA-MA and B, Z. In Figures 6-7 the PAA-MA/B and PAA-MA/Z surface seems very rough, granule and homogeneous. On the other hand, SEM photographs of PAA-MA/B and PAA-MA/Z that have the higher metal adsorption show that it has more pores and surfaces. This large pores reduce diffusional resistance and facilitate mass transfer because of large inner surface area. This also provides higher metal ions removal capacity. This result could be confirmed by the large surface area verified by the BET analysis.

Surface area measurements (BET)

The results of adsorption surface area and porosity measurements were provided in Table 9. Both adsorbents had nanoporosity with reference to the IUPAC classification, since their pore diameter values are within the range of 2-50 nm. The surface area and pore volume of the PAA-MA/B and PAA-MA/Z were significantly different from PAA-MA, but PAA-MA/B had a wider BET surface area than PAA-MA. Specific surface area of the PAA-MA/B and PAA-MA/Z composites were found to be 5.9 m^2/g, 4.6 m^2/g, respectively. It can be concluded that the B and Z incorporated composites have a nanoparticle interior surrounded by a reasonably rough surface. In addition, these nanoparticle reduce diffusional resistance and facilitate mass transfer because of hight internal surface area.

Swelling studies

The highest swelling degree were observed for the PAA-MA/B and PAA-MA/Z containing 2:1 (mass ratio PAA-MA:B/Z) bentonite and zeolite in each group of PAA-MA/B and PAA-MA/Z. When bentonite and zeolite content in a sample exceeded 2:1 (mass ratio PAA-MA:B/Z), swelling degree increased gradually. Effect of bentonite and zeolite content is clearly seen in Table 10 for the PAA-MA/B and PAA-MA/Z. It is well known that the swelling of hydrogel is induced by electrostatic repulsion of the ionic charges of its network [23]. The ionic charge content is important. Maleic acid contains many ionic units (-COOH). The magnitude of swelling were found to be 1150% for B, 15% for Z, 1035% for PAA-MA, 3340% for PAA-MA/B and 1340% for PAA-MA/Z. By considering the PAA-MA contents of the PAA-MA/B and PAA-MA/Z (0.67 of 1 g), it is obvious that the swelling property of the PAA-MA/B and PAA-MA/Z increased. It should be also noted that these composites (PAA,MA/B and PAA-MA/Z) are quite rigid, and strong enough due to the highly network structure, therefore they are suitable for reusable applications.

pH at the point of zero charge (PZC)

Figures 8-10 show the variation in ΔpH as a function of pHi in 0.1 M KNO_3 as a background electrolyte. The point of zero charge describes the condition when the electrical charge density on a surface is zero. The pH of point of zero charge (pHPZC) of an composites depends on the chemical and electronic properties of the functional groups on its surface, components and is a good indicator of these properties. Table 11 gives the pHPZC values of PAA-MA and PAA-MA/B and PAA-MA/Z. The PZC of PAA-MA and PAA-MA/B and PAA-MA/Z were found at pH of 6.2, 6.5 and 6.0, respectively. The total content of the acid groups is bigger than the content of the basic groups, making the pH the point of charge zero, pHPZC. The PAA-MA has a pHPZC light acid with a value of 6.2. PAA-MA/Z, the pHPZC of the composite decreased markedly due to an increase in the amount of the surface acidic oxygen-containing groups. This means that Bentonite and zeolite of the been modified PAA-MA at amount of acidic groups. As shown in Table 11, composites will readily adsorb protons from solution, whereas those with acidic character and lower pH PZC value will release protons to form net negative surface charges, which is benefcial for the aqueous metal adsorption [29].

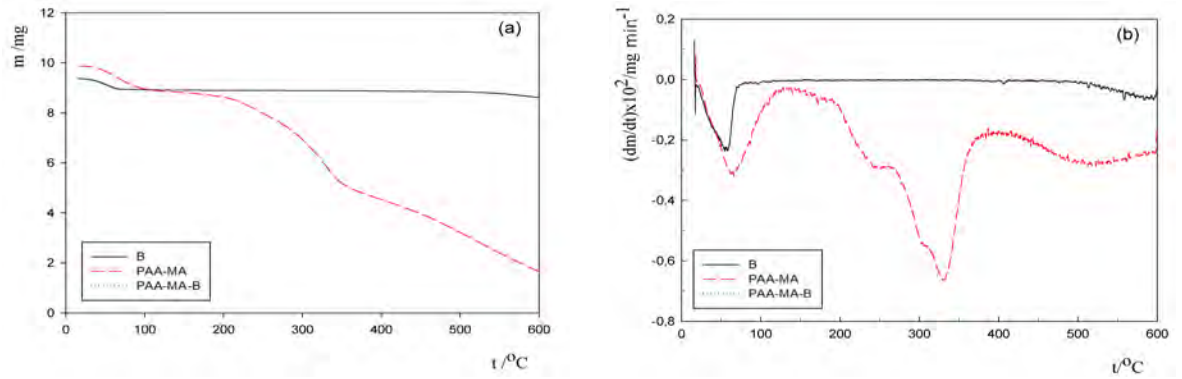

Figure 4. The derivative TGA curves (heating rate: 10 ^{o}Cmin^{-1} under static air) of B, PAA-MA and PAA-MA/B.

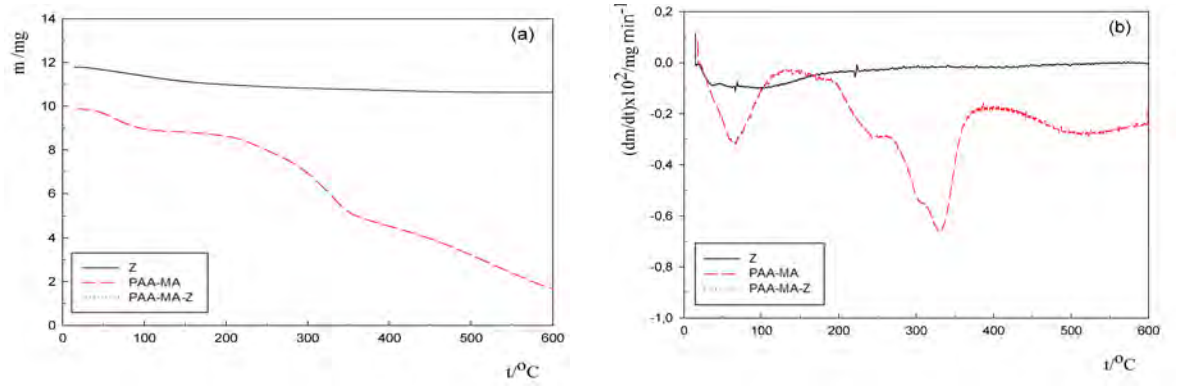

Figure 5. The derivative TGA curves (heating rate: 10 ^{o}Cmin^{-1} under static air) of Z, PAA-MA and PAA-MA/Z.

It is well known that pH is important for adsorption of metal cations as well as ionizable organic compounds on chemically active sites on the adsorbent surface [29]. The point of zero charge (PZC), an important characteristic of minerals, is usually used to define the state of the surface of a dispersed solid phase at the solid electrolyte solution surface. Thus, the PZC of a specific mineral is the pH value (pHPZC) at which negative and positive surface concentrations are equal, i.e. surface charge, pH_{pzc} = 0. The surface charge is negative at pH > pH_{pzc} and positive at pH < pH_{pzc} [28,29]. The results of FT-IR, TGA, SEM, BET-porosity and SYN analysis presented certain evidences for the formation of composites, it was impressed that the composites were the mixtures composed of two phases composing of organic (PAA-MA) and inorganic (B or Z) phases rather than the formation of polymer/mineral hybrid.

CONCLUSION

This study introduced the composite of B and Z with PAA-MA as alternative adsorbent materials. B or Z was the supportive components for PAA-MA, the preparation and characterization of PAA-MA/B and PAA-MA/Z composites. The results of FT-IR, TGA, SEM, BET-porosity and PZC analysis presented certain evidences for the formation of composites, it was impressed that the composites were the mixtures composed of two phases composing of organic (PAA-MA) and inorganic (B or Z) phases rather than the formation of polymer/mineral hybrid.

In consequence, the studied features of PAA-MA/B and PAA-MA/Z suggest that the materials should be considered as a new adsorbent. It is envisaged that the use of B and Z in PAA-MA will enhance practicality and effectiveness of B and Z in separation and removal procedures.

ACKNOWLEDGEMENT

This work was supported by The Research Fund of Cumhuriyet University (CUBAP, Project no: F-230) to which the authors are grateful.

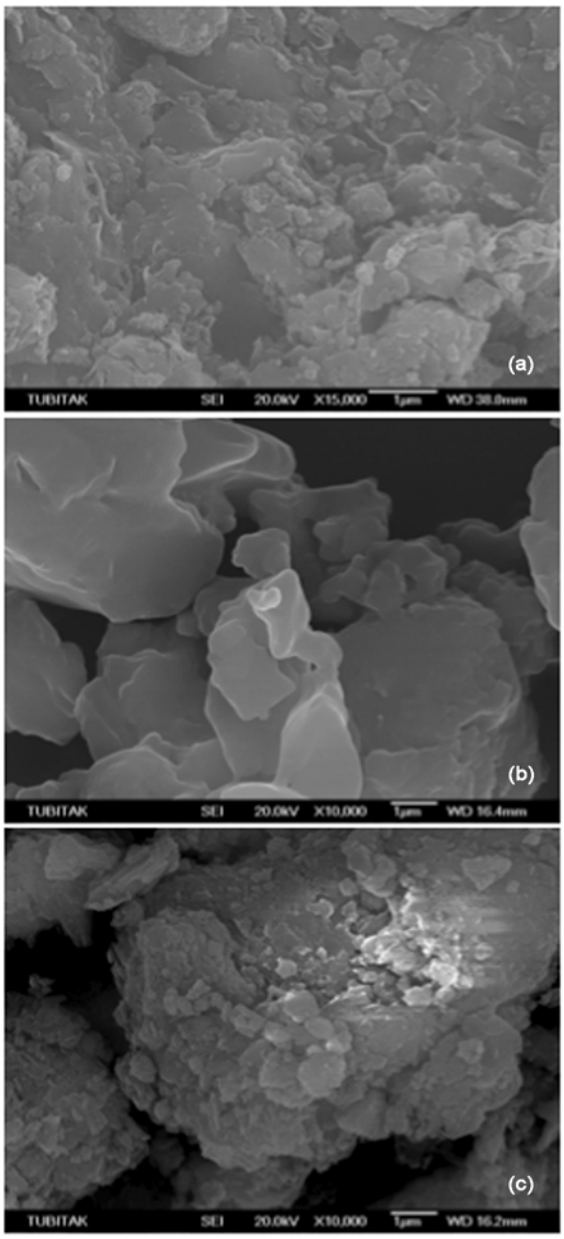

Figure 6. SEM photographs of B (a), PAA/MA (b) and PAA-MA/B (c).

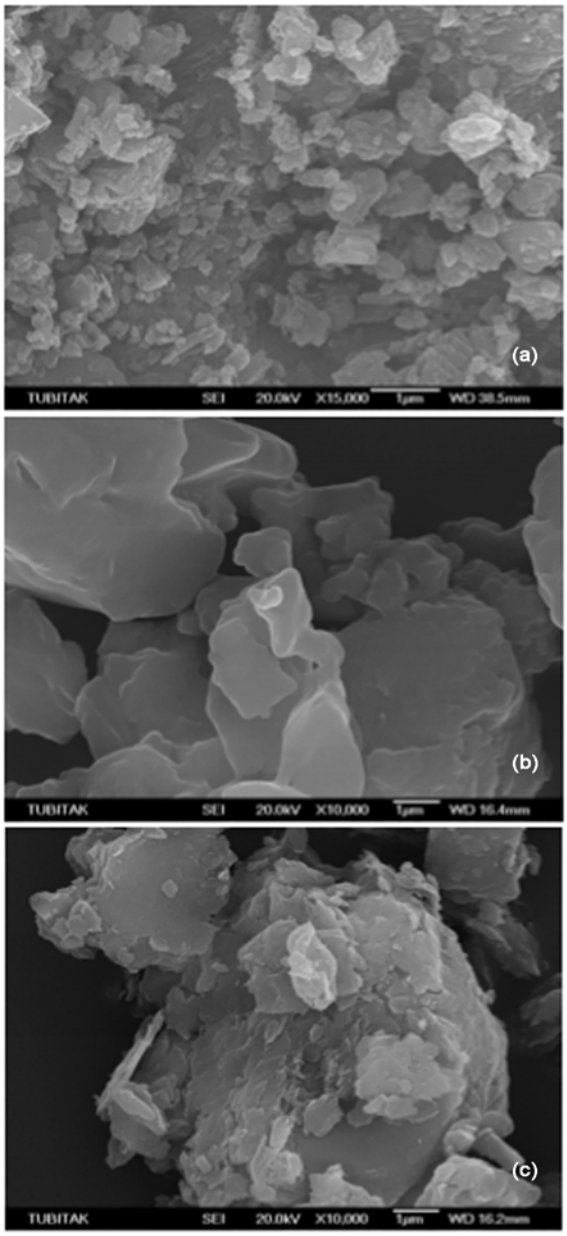

Figure 7. SEM photographs of B (a), PAA/MA (b) and PAA-MA/B (c).

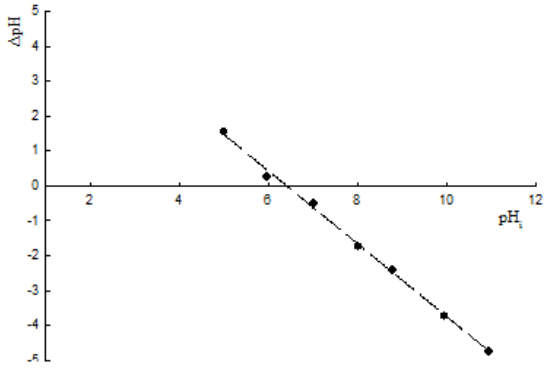

Figure 8. PZC of PAA-MA and in the pH range 2-11 at 298 K ($\Delta pH=-1.04\ pH_i=6.68$, $R^2=0.997$, $p < 0.05$).

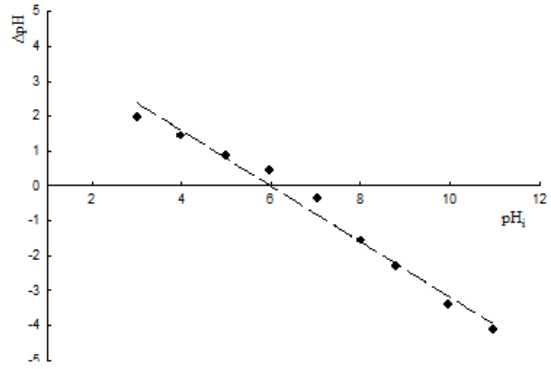

Figure 9. Surface groups and pHPZC of PAA-MA/B ($\Delta pH=-0.80\ pH_i=4.77$, $R^2=0.982$, $p < 0.05$).

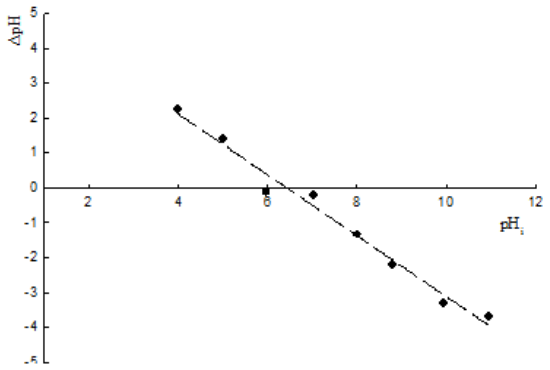

Figure 10. PZC of PAA-MA/Z ($\Delta pH=-0.87pH_i=5.61$, $R^2=0.983$, $p < 0.05$).

REFERENCES

1. T.V. Budtova, I.E. Suleıman, S.Y. Frenkel, On the swelling of polyelectrolyte hydrogels in solutions of lınear-polymers, Vyskom. Sodeny. 35 (1993) 93.
2. H.N. Oztop, D. Saraydin, E. Karadag, Y. Caldıran, O. Güven, Influence of some aromatic amino acids on the swelling behavior of acrylamide/maleic acid hydrogel, Polym. Bull. 40 (1998) 575.
3. R. Inam, Y. Gumus, T. Caykara, Competitive removal of Pb^{2+}, Cd^{2+}, and Zn^{2+} by poly(acrylamide-co-maleic acid) hydrogels/differential pulse polarographic determination, J. Appl. Polym. Sci. 94 (2004) 2401.
4. E. Karadağ, O.B. Uzum, D. Saraydin, Swelling equilibria and dye adsorption studies of chemically crosslinked superabsorbent acrylamide/maleic acid hydrogels, Eur. Polym J. 38 (2002) 2133.
5. H. Kaşgöz, New sorbent hydrogels for removal of acidic dyes and metal ions from aqueous solutions, Poly. Bull. 56 (2006) 517.
6. P.B. Messersmith, F. Znidarsich, Synthesis and LCST behavior of thermally responsive poly(N-isopropyl acrylamide)/layered silicate nanocomposites, Mat. Res. Soc. Symp. Proc. 457 (1997) 507.
7. J.H. Wu, J.M. Lin, M. Zhou, C.R. Wei, Synthesis and properties of starch-graft-polyacrylamide/clay superabsorbent composite. Macromolecules. 21 (2000) 1032.
8. J.M. Lin, J.H. Wu, Z.F. Yang, M.L. Pu, Synthesis and properties of poly(acrylic acid)/mica superabsorbent nanocomposite. Macromolecules. 22 (2001) 422.
9. W.A. Zhang, W. Luo, Y.E. Fang, Synthesis and properties of a novel hydrogel nanocomposites. Mater. Lett. 59 (2005) 2876.
10. K. Haraguchi, T. Takehisa, Nanocomposite hydrogels: a unique organic–inorganic network structure with extraordinary mechanical, optical, and swelling/de-swelling properties. Adv. Mater. 14 (2002) 1120.
11. K. Haraguchi, T. Takehisa, S. Fan, Effects of clay content on the properties of nanocomposite hydrogels composed of poly(N-isopropylacrylamide) and clay. Macromolecules, 35 (2002) 10162.
12. A. Denizli, R. Say, B. Garipcan, S. Patır, Methacryloylamidoglutamic acid functionalized poly(2-hydroxyethyl methacrylate) beads for UO_2^{2+} removal, React. Funct. polym. 58 (2004) 123.
13. X. Yuanqing, P. Zhiqin, A new polymer/clay nano-composite hydrogel with improved response rate and tensile mechanical properties, Eur. Polym. J. 42 (2006) 2125.
14. U.A. Atay, Ammonia removal from waste waters by the use of zeolite. MSc. Thesis, Cumhuriyet University, Sivas, Turkey. 2002.
15. B. Demirel, O. Yenigun, T.T. Onay, Anaerobic treatment of dairy wastewaters: a review, Process Biochem. 40 (2005) 2583.
16. P. Akkas, O. Guven, Enhancement of uranyl ion uptake by prestructuring of acrylamide-maleic acid hydrogels, J. Appl. Polym. Sci. 78 (2000) 284.
17. R. Akkaya, U. Ulusoy, Adsorptive features of chitosan entrapped in polyacrylamide hydrogel for Pb^{2+}, UO_2^{2+} and Th^{4+}, J. Hazard. Mater, 151 (2008) 380.
18. M. Mullet, P. Fievet, A. Szymczyk, A. Foissy, J.C. Reggiani, J. Pagetti, A simple and accurate determination of the point of zero charge of ceramic membranes, Desalination, 121 (1999) 41.
19. I. Smiciklas, A. Onjia, S. Raicevic, D. Janackovic, M. Mitric, Factors influencing the removal of divalent cations by hydroxyapatite, J.Hazard. Mat. 152 (2008) 876.
20. U. Ulusoy, R. Akkaya, Adsorptive features of polyacrylamide–apatite composite for Pb^{2+}, UO_2^{2+} and Th^{4+}, J. Hazard. Mater. 163 (2009) 98.
21. S.E. Abdel-Aal, Synthesis of copolymeric hydrogels using gamma radiation and their utilization in the removal of some dyes in wastwater, J. Appl. Poly. Sci.102 (2006) 3720.
22. J. Madejova, FTIR techniques in clay mineral studies, Vib. Spectrosc. 31 (2003) 1.
23. B. Zhang, W. Dai, X.C. Ye, W.Y. Hou, Y. Xie, Solution-phase synthesis and electrochemical hydrogen storage of ultra-long single-crystal selenium submicrotubes, J. Physical Chem. B. 109 (2005) 22830.
24. M. Alexandre, P. Dubois, Polymer-layered silicate nanocomposites: preparation, properties and uses of a new class of materials, Mat. Sci. Eng. R. 28 (2000) 1.
25. D. Saraydin, D. Solpan, Y. Isikver, S. Ekici, O. Güven, Radiation crosslinked poly(acrylamide/2-hydroxypropyl methacrylate/maleic acid) and their usability in the uptake of uranium, Macromol. Sci-A. A39 (2002) 969.
26. J.J. Gulicovski, L.C. Cerovic, S.K. Milonjic, I.G. Popovic, Adsorption of itaconic acid from aqueous solutions onto alumina, J. Serb. Chem. Soc. 73 (2008) 825.
27. L. Giraldo, J.C. Moreno, Immersion enthalpy and the constants of Langmuir model in the 3-chloro phenol adsorption on activated carbon, J Therm. Anal. Calorim. 100 (2010) 695.
28. A. Dakovic, M. Kragovic, G.E. Rottinghaus, Z. Sekulic, S. Milicevic, S.K. Milonjic, S. Zaric, N-fluence of natural zeolitic tuff and organozeolites surface charge on sorption of ionizable fumonisin B-1, Colloid. Surface B, 76 (2010) 272.
29. J.J. Gulicovski, L.S. Cerovic, S.K. Milonjin, Point of zero charge and isoelectric point of alumina, Mater. Manuf. Process. 23 (2008) 615.